Above- and Belowground Plant Mercury Dynamics in a Salt Marsh Estuary in Massachusetts, USA

Ting Wang[1], Buyun Du[1], Inke Forbrich[2], Jun Zhou[1], Joshua Polen[1], Elsie M. Sunderland[3], Prentiss H. Balcom[3], Celia Chen[4], Daniel Obrist[1,5]

[1]Department of Environmental, Earth, and Atmospheric Sciences, University of Massachusetts Lowell, Lowell, MA 01854, USA

[2]Marine Biological Laboratory, Woods Hole, MA 02543, USA

[3]Harvard John A. Paulson School of Engineering and Applied Sciences, Harvard University, Cambridge, MA 02138, USA

[4]Department of Biological Sciences, Dartmouth College, Hanover, NH 03755, USA

[5]Division of Agriculture and Natural Resources, University of California, Davis, CA 95618, USA

Correspondence to: Daniel Obrist (daniel_obrist@uml.edu)

Supplementary Documents

Hg Isotope Mixing Model

A ternary isotope mixing model was used to estimate the fractions of Hg in salt marsh plant leaves derived from the three dominant end-member Hg sources (medians). These sources include: (1) salt marsh plants roots, where the median Hg isotope composition of marsh plant roots collected in this study for δ^{202}Hg is -0.69‰ (ranging from -0.75‰ to -0.66‰, n =4), for Δ^{200}Hg is 0.03‰ (ranging from -0.01‰ and 0.04‰), and for Δ^{199}Hg is 0.17 ‰ (ranging from 0.11‰ to 0.22‰); (2) atmospheric GEM, where published upland foliage Hg isotopic signatures are used to represent GEM taken up by plants from atmospheric GEM (on average 88% [79-100%, IQR]) (Zhou et al., 2021). The median Hg isotope compositions of upland foliage for δ^{202}Hg is -2.84‰, for Δ^{199}Hg is -0.37‰, and for Δ^{200}Hg is -0.02‰ (n = 120) (review by Zhou et al., 2021); and (3) precipitation, where the median Hg isotope composition of precipitation is used from previous published data points (δ^{202}Hg: -0.30‰, Δ^{199}Hg: 0.4‰, Δ^{200}Hg: 0.17‰ n = 106) (Table S4) (Jiskra et al., 2021). The calculation equations are as followings:

$$\Delta^{200}Hg_{vegetation} = f_{atm\_GEM}\Delta^{200}Hg_{atm\_GEM} + f_{root}\Delta^{200}Hg_{root} + f_{prep\_Hg(II)}\Delta^{200}Hg_{prep\_Hg(II)} \quad (1)$$

$$\delta^{202}Hg_{vegetation} = f_{atm\_GEM}\delta^{202}Hg_{atm\_GEM} + f_{root}\delta^{202}Hg_{root} + f_{prep\_Hg(II)}\delta^{202}Hg_{prep\_Hg(II)} \quad (2)$$

$$f_{atm\_GEM} + f_{root} + +f_{prep\_Hg(II)} = 1 \quad (3)$$

We used an excel model to estimate the respective fractions. Our initial constraints were to start with a fraction of atmospheric GEM uptake (based on upland foliage data) as 50%, then adjusted the fractions of roots uptake and precipitation deposition stepwise to calculate values of δ^{202}Hg and Δ^{200}Hg in salt marsh plant leaves. We modified the respective fractions (increasing and decreasing) until we found best estimates of δ^{202}Hg and Δ^{200}Hg corresponding to salt marsh plant leaves (medians value).

Industrial Hg Isotopic Signatures

The isotopic signatures of industrial Hg are characterized by a wide range of negative δ^{202}Hg values, while Δ^{199}Hg and Δ^{200}Hg values are generally close to zero or positive (Fig S3, Table S4). For example, urban soil Hg signatures in Beijing, China showed δ^{202}Hg values between -1.14‰ and -0.59‰, Δ^{199}Hg values between 0.03‰ and 0.10‰ and Δ^{200}Hg values between 0.02‰ and 0.04‰ (Huang et al., 2016); contaminated coastal marine sediments along Northeastern USA. showed δ^{202}Hg values between -0.82‰ and -0.38‰, Δ^{199}Hg values between 0.01‰ and 0.18‰ and Δ^{200}Hg values between -0.04‰ and 0.02‰ (Kwon et al., 2014);

industrial sources impacted sediments of Great Lakes USA showed δ^{202}Hg values between -1.28‰ and -0.14‰, Δ^{199}Hg values between -0.04‰ and 0.11‰ and Δ^{200}Hg values between -0.02‰ and 0.09‰ (Lepak et al., 2015); and in Northeastern France showed δ^{202}Hg values between -0.72‰ and -0.16‰ and Δ^{199}Hg values between -0.08‰ and 0.09‰ (Estrade et al., 2011). Similarly, Hg isotopic signatures in historic industrial influenced bank soils of Virginia, USA, showed δ^{202}Hg values between -1.05‰ and -0.18‰, Δ^{199}Hg values between 0.00‰ and 0.10‰, and Δ^{200}Hg values between -0.02‰ and 0.03‰ (Washburn et al., 2017).

Table S1. Hg concentrations, dry weights, and Hg mass of above- and belowground biomass and surface soils of the two plant dominated communities.

Items	Plant species	Hg concentration µg kg^{-1}	STD	Dry Weight g m^{-2}	STD	Hg mass µg m^{-2}	STD
Live root	*S. alterniflora*	84.5	47.0	278	61	22.0	7.9
	S. patens	258.9	70.3	444	87	118.0	53.8
Live rhizome	*S. alterniflora*	27.9	1.1	598	44	18.8	3.5
	S. patens	46.6	14.2	987	87	57.4	2.9
Senesced biomass_0-20cm	*S. alterniflora*	318.0	30.1	54	9	1912.3	606.3
	S. patens	323.3	135.4	6537	611	2068.0	1017.3
Mineral and humus_0-20cm	*S. patens*	272.3	11.6				
Bulk soil_0-20cm	*S. alterniflora*	194.6	28.3	71078	6794	13925.8	3334.7
	S. patens	171.2	72.1	53193	10143	9470.1	5570.3
Senesced biomass_20-40cm	*S. alterniflora*	639.1	337.1	2660	3704	3077.7	1512.2
	S. patens	263.1	208.7	5119	977	1174.2	845.2
Mineral and humus_20-40cm	*S. patens*	73.1	10.2				
Bulk soil_20-40cm	*S. alterniflora*	279.1	203.8	70523	2904	19977.1	15183.1
	S. patens	159.1	122.7	55838	18002	7777.1	3986.2

Table S2. Hg concentrations, dry weights, and Hg mass of above- and belowground biomass and surface soils of the combined plant communities.

	Items	Hg concentration µg kg^{-1}	STD	Dry biomass weight g m^{-2}	STD	Hg mass µg m^{-2}	STD
Belowground	Live Root	171.7	111.9	361	114	70.0	63.7
	Live Rhizome	37.3	13.6	792	231	38.1	22.4
	Live Root and Rhizome	84.6	49.1	1,153	321	108.1	83.4
	Senesced Biomass	385.9	224.2	11,724	1,165	4,116.1	1,141.0
	Mineral and Humus	172.7	140.8	112,439	-	21,350.9	-
	Bulk Soil	202.1	117.8	125,316	25,475	25,575.1	14,408.7
Aboveground	Green Biomass	16.2	2.0	368	149	5.7	2.1
	Senesced Biomass	15.2	2.2	215	92	3.3	1.7
	Green and Senesced	-	-	583	208	9.0	3.3

Table S3. Hg isotope signatures in salt marsh plant tissues and soils and their corresponding Hg concentrations.

Item	Sample ID	THg concentration (ng g^{-1})	δ^{202}Hg (‰)	Δ^{200}Hg (‰)	Δ^{199}Hg (‰)	Δ^{201}Hg (‰)
Aboveground biomass	ABO-L-1	4.6	-1.07	0.11	0.20	0.16
	ABO-L-2	8.0	-1.61	0.06	0.43	0.26
	ABO-L-3	6.9	-1.21	0.07	0.42	0.23
	ABO-L-4	7.9	-1.29	0.04	0.32	0.11
Rhizome	BL-RHI-1	28.7	-0.70	-0.03	0.16	-0.02
	BL-RHI-2	35.0	-1.31	0.04	0.13	0.08
	BL-RHI-3	18.0	-0.80	0.02	0.15	0.11
	BL-RHI-4	36.5	-1.41	-0.05	0.22	0.09
Root	BL-ROOT1	52.4	-0.69	0.04	0.20	0.06
	BL-ROOT2	138.0	-0.75	0.04	0.22	0.08
	BL-ROOT3	93.0	-0.66	0.02	0.13	0.03
	BL-ROOT3-2	93.0	-0.73	0.01	0.14	0.01
	BL-ROOT4	308.6	-0.69	-0.01	0.11	0.07
Surface Soil	S1L1	172	-0.32	0.03	0.14	0.10
	S1L2	275	-0.41	-0.02	0.16	0.02
	S1L3-4	378	-0.42	0.01	0.17	0.01
	S2L1	220	-0.36	0.05	0.17	0.11
	S2L2	429	-0.35	0.05	0.17	0.06
	S2L3-4	373	-0.29	0.03	0.16	0.06
	S3L1	119	-0.31	-0.01	0.17	0.01
	S3L1-2	119	-0.39	0.00	0.13	0.06
	S3L2	269	-0.60	0.02	0.07	0.07
	S3L3-4	406	-0.44	0.00	0.15	0.03
	S4L1	191	-0.41	-0.01	0.15	0.00
	S4L2	349	-0.41	0.03	0.20	0.03
	S4L3-4	416	-0.42	0.00	0.11	-0.02
Deep Soil	S1L9	57	-0.51	-0.01	0.04	0.03
	S2L9	56	-0.53	0.00	0.10	0.12
	S3L9	9	-0.72	0.04	0.19	-0.02
	S4L9	19	-0.92	0.03	-0.09	-0.13
	S4L9-2	19	-0.92	0.02	-0.07	-0.12

Table S4. Hg isotopic signatures of salt marsh plants and soils (this study) and other published data.

Item	$\delta^{202}Hg$ (‰)		$\Delta^{199}Hg$ (‰)		$\Delta^{200}Hg$ (‰)		Reference
	Median	Min to Max	Median	Min to Max	Median	Min to Max	
Aboveground veg. (n=4)	-1.25	-1.61 to -1.07	0.37	0.20 to 0.43	0.06	0.04 to 0.11	this study
Rhizome (n=4)	-1.05	-1.41 to -0.70	0.16	0.13 to 0.22	-0.01	-0.05 to 0.04	this study
Root (n=4)	-0.69	-0.75 to -0.66	0.17	0.11 to 0.22	0.03	-0.01 to 0.04	this study
Root and rhizome (n=8)	-0.73	-1.41 to -0.66	0.16	0.11 to 0.22	0.02	-0.05 to 0.04	this study
Soil (n=16)	-0.42	-0.92 to -0.29	0.15	-0.02 to 0.20	0.01	-0.02 to 0.05	this study
Item	$\delta^{202}Hg$ (‰)		$\Delta^{199}Hg$ (‰)		$\Delta^{200}Hg$ (‰)		Reference
	Median	IQR*	Median	IQR	Median	IQR	
Upland veg. (n=120)	-2.84	-3.06 to -2.37	-0.37	-0.42 to -0.27	-0.02	-0.05 to 0.01	Review by Zhou et al., 2021
Rainfall (n=106)	-0.30	-0.63 to 0.03	0.40	0.21 to 0.52	0.17	0.11 to 0.22	Jiskra et al., 2021
Ocean sediment (n=92)	-0.85	-1.21 to -0.49	0.08	0.02 to 0.11	0.02	0.01 to 0.04	Jiskra et al., 2021
Ocean water total Hg (n=16)	-0.24	-0.42 to -0.04	0.06	0.02 to 0.01	0.02	-0.01 to 0.03	Jiskra et al., 2021
Atm Hg (n=220)	0.43	0.09 to 0.77	-0.20	-0.13 to -0.06	-0.05	-0.08 to -0.03	Jiskra et al., 2021
Industrial Hg (n=46)	-0.64	-0.72 to -0.42	0.02	-0.03 to 0.04	0.01	0.00 to 0.03	Estrade et al., 2011; Huang et al., 2016; Kwon et al., 2014; Lepak et al., 2015; Washburn et al., 2017

*IQR: Inter-Quartile Range

Table S5. Hg concentrations in washed and unwashed aboveground green biomass samples.

Date	*S. alterniflora* - unwashed		*S. alterniflora* - washed*		Estimated throughfall (μg kg^{-1})**
	Hg Concentration (μg kg^{-1})	STD	Hg Concentration (μg kg^{-1})	STD	
Aug-21	10.1	0.2	7.0	0.0	3.1
Sep-21	9.7	2.8	7.9	0.6	1.8
Oct-21	10.8	3.2	11.4	4.9	-0.7
Nov-21	15.8	1.2	16.2	2.6	-0.4
Average	**11.8**	**3.4**	**11.1**	**4.6**	**0.7**

Date	*S. patens*- unwashed		*S. patens*- washed*		Estimated throughfall (μg kg^{-1})**
	Hg Concentration (μg kg^{-1})	STD	Hg Concentration (μg kg^{-1})	STD	
Aug-21	8.6	1.0	7.0	0.6	1.5
Sep-21	10.9	2.1	9.0	1.0	1.9
Oct-21	12.8	1.7	11.8	1.0	1.0
Nov-21	18.8	3.2	16.2	1.7	2.6
Average	**13.0**	**4.3**	**11.3**	**3.7**	**1.8**

* Assumed structural Hg (not subject to throughfall).
** Throughfall is estimated as amount of Hg washed off from aboveground tissues

Table S6. Comparing Hg concentrations in aboveground plants and roots with other contaminated and non-contaminated marsh vegetation.

Study sites	Plant Species	Session	THg µg kg^{-1}	Reference	Note
Piles Creek, NJ, USA	*S. alterniflora*	Aboveground	160 ±70.0	Kraus et al., 1986	Contamination
Hackensack Meadowlands, NJ, USA	*Phragmites australis*	Aboveground	18-30	Windham et al., 2001	Contamination
	S. alterniflora		30-90		
Ria de Aveiro Coastal Lagoon, Portugal	*Halimione portulacoides*	Aboveground	88-970	Anjum et al., 2011	Contamination
		Root	248-9,957		
	Juncus maritimus Collected	Aboveground	23-268		
		Root	417-23,330		
Tagus estuary, Portugal	*Halimione Portulacoides*	Aboveground	53 ± 12	Canário et al., 2017	Contamination
	Sarcorcornia fruticosa		12 ± 7		
	S. maritima		23 ± 9		
Tagus estuary, Portugal	*Halimione Portulacoides*	Root	1124 ± 21	Canário et al., 2017	Contamination
	Sarcorcornia fruticosa		873 ± 39		
	S. maritima		1031 ± 42		
Salt marsh, northern Spain	*Juncus maritimus*	Aboveground	10–194	Garcia-Ordiales et al., 2020	Contamination
		Root	58–2,522		
Yangtze River estuary, China	overall	Aboveground	12.5 ± 2.5 (9.0-17.4)	Wang et al., 2021	Contamination
	S. alterniflora		10.2 ± 0.9		
	P. australis		12.6 ± 1.8		
	S. marqueter		14.7 ± 1.8		
Yangtze River estuary, China	*S. alterniflora*	Root	36.6±6.7	Wang et al., 2021	Contamination
	P. australis		9.9±2.9		
	S. marqueter		34.0±4.7		

Table S6. Comparing Hg concentrations in aboveground and roots with other contaminated and non-contaminated marsh vegetation (Continued).

Study sites	Plant Species	Session	THg μg kg^{-1}	Reference	Note
Big Sheepshead Creek, NJ, USA	*S. alterniflora*	Aboveground	20 ±0	Kraus et al., 1986	No contamination
Great Bay Estuary, NH, USA	*S. alterniflora*	Aboveground	4.61-33.4	Heller and Weber, 1998	No contamination
Ria de Aveiro Coastal Lagoon, Portugal	*Halimione portulacoides*	Aboveground	32-79	Anjum et al., 2011	No Contamination
		Root	153-802		
	Juncus maritimus Collected	Aboveground	3-24		
		Root	152-358		
Parker River, MA, USA	Overall (n=56)	Aboveground	7.6±5.5* (0.8-24.0)	This study	No contamination
	S. alterniflora		5.1±3.3* (0.8-11.7)		
	S. patens		9.7±6.6* (2.0-24.0)		
Parker River, MA, USA	Overall (n=4)	Root	171.7±111.9	This study	No contamination
	S. alterniflora		84.5±47.0		
	S. patens		258.9±70.3		

* Range across growing season and late season maximum values

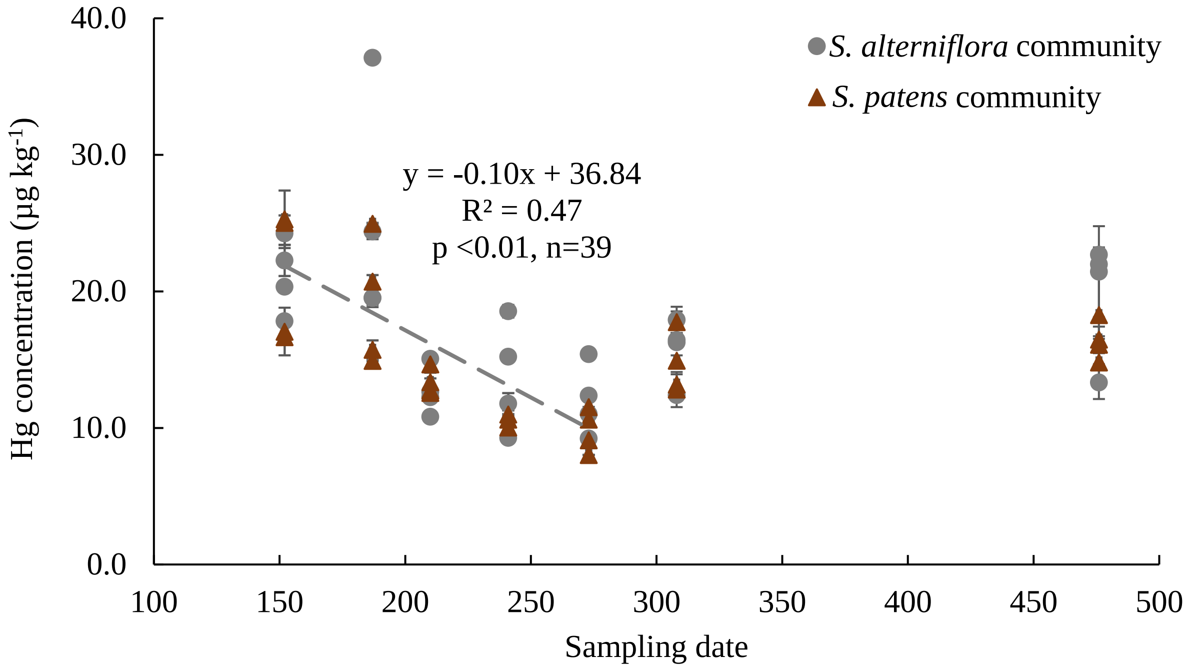

68

69 **Figure S1. Hg concentrations of seasonal patterns of senesced *S. alterniflora* and *S. patens* communities with sampling dates in 2021.**
70 **Grey circles denote of senesced *S. alterniflora* communities, and brown triangles denote of senesced *S. patens* communities. Standard**
71 **errors indicate four replicates.**

72

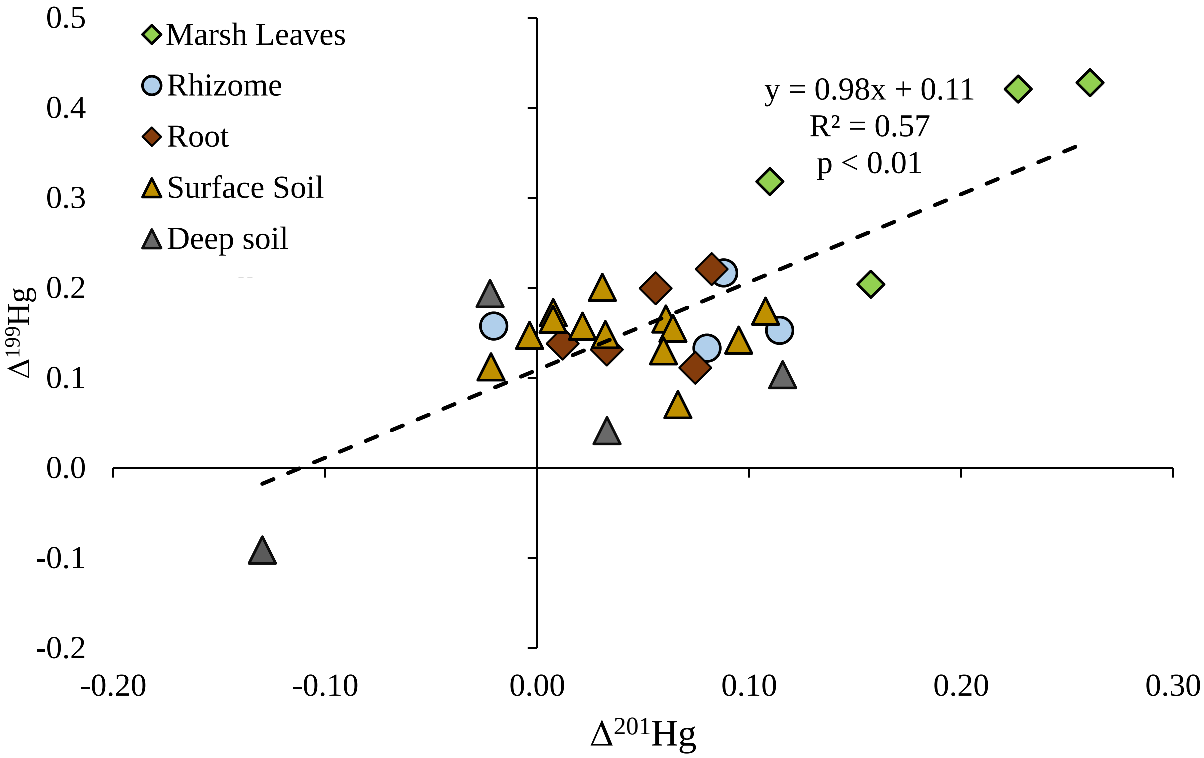

Figure S2. Relationship between Δ^{201}Hg and Δ^{199}Hg of all salt marsh samples. Different color symbols indicate different types of salt marsh samples.

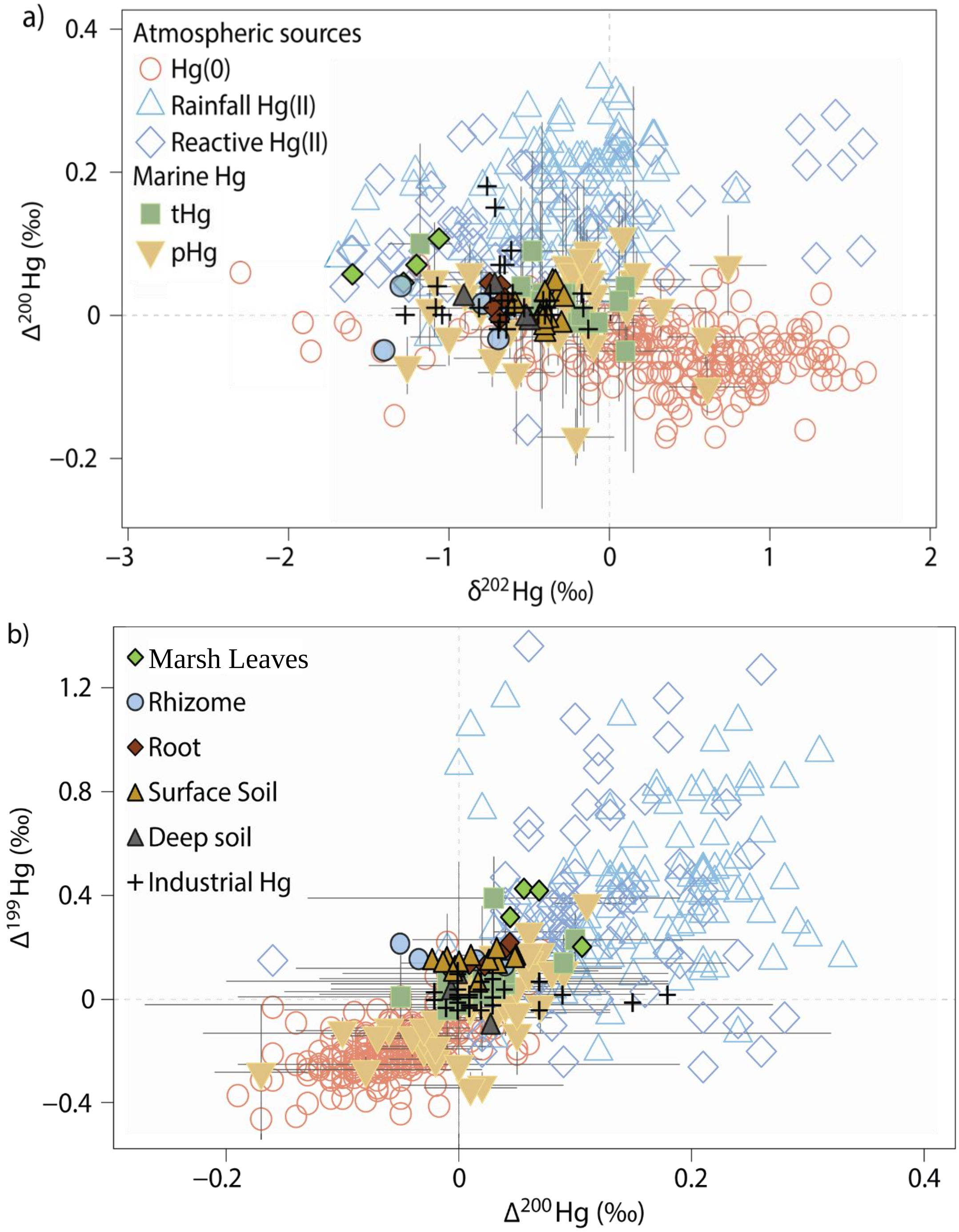

Figure S3. Relationships of Δ202Hg and Δ199Hg (a), and of Δ200Hg and Δ199Hg (b) of previous published marine Hg sources, atmospheric Hg sources (Jiskra et al., 2021), industrial Hg polluted soils and sediments (Estrade et al., 2011; Huang et al., 2016; Kwon et al., 2014; Lepak et al., 2015; Washburn et al., 2017), along with Hg signatures of marsh plants and soils in this study. Different color symbols indicate different marsh samples.

References

Anjum, N. A., Ahmad, I., Válega, M., Pacheco, M., Figueira, E., Duarte, A. C., & Pereira, E. (2011). Impact of seasonal fluctuations on the sediment-mercury, its accumulation and partitioning in Halimione portulacoides and Juncus maritimus collected from Ria de Aveiro coastal lagoon (Portugal). *Water, Air, and Soil Pollution*, *222*(1–4), 1–15. https://doi.org/10.1007/s11270-011-0799-4

Canário, J., Poissant, L., Pilote, M., Caetano, M., Hintelmann, H., & O'Driscoll, N. J. (2017). Salt-marsh plants as potential sources of Hg0 into the atmosphere. *Atmospheric Environment*, *152*, 458–464. https://doi.org/10.1016/j.atmosenv.2017.01.011

Estrade, N., Carignan, J., & Donard, O. F. X. (2011). Tracing and quantifying anthropogenic mercury sources in soils of northern France using isotopic signatures. *Environmental Science and Technology*, *45*(4), 1235–1242. https://doi.org/10.1021/es1026823

Garcia-Ordiales, E., Roqueñí, N., & Loredo, J. (2020). Mercury bioaccumulation by Juncus maritimus grown in a Hg contaminated salt marsh (northern Spain). *Marine Chemistry*, *226*, 103859. https://doi.org/10.1016/j.marchem.2020.103859

Heller, A. A., & Weber, J. H. (1998). Seasonal study of speciation of mercury(II) and monomethylmercury in Spartina alterniflora from the Great Bay Estuary, NH. *Science of the Total Environment*, *221*(2–3), 181–188. https://doi.org/10.1016/S0048-9697(98)00285-X

Huang, Q., Chen, J., Huang, W., Fu, P., Guinot, B., Feng, X., … Yu, B. (2016). Isotopic composition for source identification of mercury in atmospheric fine particles. *Atmospheric Chemistry and Physics*, *16*(18), 11773–11786. https://doi.org/10.5194/acp-16-11773-2016

Jiskra, M., Heimbürger-Boavida, L.-E., Desgranges, M.-M., Petrova, M. V., Dufour, A., Ferreira-Araujo, B., … Sonke, J. E. (2021). Mercury stable isotopes constrain atmospheric sources to the ocean. *Nature*, *597*(7878), 678–682. https://doi.org/10.1038/s41586-021-03859-8

Kraus, M. L., Weis, P., & Crow, J. H. (1986). The excretion of heavy metals by the salt marsh cord grass,Spartina alterniflora, and Spartina's role in mercury cycling. *Marine Environmental Research*, *20*(4), 307–316. https://doi.org/10.1016/0141-1136(86)90056-5

Kwon, S. Y., Blum, J. D., Chen, C. Y., Meattey, D. E., & Mason, R. P. (2014). Mercury isotope study of sources and exposure pathways of methylmercury in estuarine food webs in the northeastern U.S. *Environmental Science and Technology*, *48*(17), 10089–10097. https://doi.org/10.1021/es5020554

Lepak, R. F., Yin, R., Krabbenhoft, D. P., Ogorek, J. M., Dewild, J. F., Holsen, T. M., & Hurley, J. P. (2015). Use of Stable Isotope Signatures to Determine Mercury Sources in the Great Lakes. *Environmental Science and Technology Letters*, *2*(12), 335–341. https://doi.org/10.1021/acs.estlett.5b00277

Wang, Y., Wang, Z., Zheng, X., & Zhou, L. (2021). Influence of Spartina alterniflora invasion on mercury storage and methylation in the sediments of Yangtze River estuarine wetlands. *Estuarine, Coastal and Shelf Science*, *265*(June 2021), 107717. https://doi.org/10.1016/j.ecss.2021.107717

Washburn, S. J., Blum, J. D., Demers, J. D., Kurz, A. Y., & Landis, R. C. (2017). Isotopic Characterization of Mercury

Downstream of Historic Industrial Contamination in the South River, Virginia. *Environmental Science and Technology*, *51*(19), 10965–10973. https://doi.org/10.1021/acs.est.7b02577

Weis, J. S., & Weis, P. (2004). Metal uptake, transport and release by wetland plants: implications for phytoremediation and restoration. *Environment International*, *30*(5), 685–700. https://doi.org/10.1016/j.envint.2003.11.002

Windham, L, Weis, J. ., & Weis, P. (2003). Uptake and distribution of metals in two dominant salt marsh macrophytes, Spartina alterniflora (cordgrass) and Phragmites australis (common reed). *Estuarine, Coastal and Shelf Science*, *56*(1), 63–72. https://doi.org/10.1016/S0272-7714(02)00121-X

Windham, Lisamarie, Weis, J. S., & Weis, P. (2001). Patterns and processes of mercury release from leaves of two dominant salt marsh macrophytes, Phragmites australis and Spartina alterniflora. *Estuaries*, *24*(6 A), 787–795. https://doi.org/10.2307/1353170

Zhou, J., Obrist, D., Dastoor, A., Jiskra, M., & Ryjkov, A. (2021). Vegetation uptake of mercury and impacts on global cycling. *Nature Reviews Earth & Environment*, *2*(4), 269–284. https://doi.org/10.1038/s43017-021-00146-y